Journal of Information Systems Engineering and Management
2025, 10(11s)
e-ISSN: 2468-4376
https://www.jisem-journal.com/

Research Article

Dual Band Metamaterial Absorber for L and S Band Applications

Jigar M. Patel[1], Rahul D. Mehta [2,*]
[1]*Research Scholar, Electronics & Communication Engineering, Gujarat Technological University, Ahmedabad, Gujarat, India.*
[2]*Electronics & Communication Engineering, Government Engineering College, Rajkot, Gujarat Technological University, Ahmedabad, Gujarat, India*
[*]*Corresponding Author: Rahul D. Mehta (email: rdmehta@hotmail.com)*

ARTICLE INFO

Received: 08 Nov 2024

Revised: 24 Dec 2024

Accepted: 15 Jan 2025

ABSTRACT

Introduction: This paper introduces a novel metamaterial absorber designed for, L-band, and S-band applications. Methods: The unit cell features a modified square-shaped double slit resonator printed on a dielectric substrate and supported by a copper layer. The absorber is extremely thin, with a total thickness of just 1.6 mm. It utilizes an FR4 epoxy dielectric substrate (εr = 4.4, tanδ = 0.02) with a thickness of 1.6 mm. Results: The absorption characteristics of the device are analyzed using Ansys HFSS, showing absorption peaks at 3 GHz, and 6.9 GHz for the S and C bands, respectively. The average absorption exceeds 90%, and the MMA structure's symmetric design ensures it remains effective across a broad range of incident angles. Design is manufactured and tested for different thickness and absorber dimensions. Comparative Analysis of simulated and manufactured design is presented in the result part. Conclusions: This makes it well-suited for applications such as aircraft surveillance, satellite navigation and radars.

Keywords: Dual Band, Metamaterial, Absorber, L band, S band

1 INTRODUCTION

Electromagnetic (EM) wave absorbers have diverse applications, including electromagnetic cloaking [1], low-radar-cross-section materials [2], sensing [3], photovoltaic and thermal photovoltaic systems [4], metal–insulator–metal structures [5], and perfect absorbers [6-8]. Among these, the most crucial use of metamaterial (MM) absorbers is in stealth technology, which is essential for military operations. The primary goal of stealth technology is to minimize signal detection or to send countermeasure signals. Consequently, researchers focus on reducing radar wave scattering and reflection from object surfaces to evade radar detection systems. Radar-absorbing surfaces enhance stealth technology by improving its performance. Furthermore, EM wave absorbers are valued for their broadband absorption capabilities and polarization-angle-insensitivity. Nowadays, achieving polarization independence in MM absorbers is relatively straightforward with symmetric structures [9-11]. Additionally, incidence-angle insensitivity can be achieved through innovative unit cell geometries such as split-ring-cross resonators [12], circular sectors [13-14], and surrounding via arrays [15]. Despite these advancements, the bandwidth of MM absorbers often remains narrow. To address this, researchers have explored various methods to extend bandwidth, including incorporating multiple resonators with different geometries in a single unit cell, combining resonators of the same shape but different sizes, using composite materials for high absorption, and adding impedance layers or stacking multiple layers. However, most existing broadband MM absorbers are effective only under normal incidence, with their performance degrading at wider oblique angles. For practical applications, an MM absorber must offer high absorption across a broad frequency range and at various incidence angles.

In this paper, we present a novel dual band double slit SRR (DSS) cell as an MMA unit cell designed for wide-incidence-angle absorption. The proposed MM absorber is implemented in a single layer, and its performance under both normal and oblique incidences is demonstrated through full-wave simulations.

2 DESIGN AND METHODOLOGY

2.1 Unit cell design

Our MMA consists of three layers: two metallic layers made of copper and one dielectric layer made of FR-4. The top front features a copper patch with a DSS cell and a conductivity of 5.8×10^{-7} S/m, as illustrated in Fig. 1(a). The backside also has a copper patch, as shown in Fig. 1(b). The copper layers on the front and back are separated by the FR-4 dielectric material, which is ideal for this application, as demonstrated in Fig. 1(c). Top of Form Figures 1(a) and 1(b) show the top and perspective views of the proposed MM unit cell, respectively. This unit cell is based on a square-loop resonator design. The resonant frequency of the square-loop resonator depends on its effective inductance and capacitance. Thus, increasing the effective inductance can lower the resonant frequency. In this design, a lumped inductor is incorporated into the square-loop resonator. To maintain symmetrical geometry, four inductors are placed on each side of the square loop. This configuration ensures that absorptivity remains constant even if the polarization of the incident wave changes.

Figure 1(c) depicts the equivalent transmission line model of the proposed unit cell. Here, Z_o and Z_d represent the characteristic impedances of air and the dielectric substrate, respectively. The square-loop resonator is modelled as a series combination of resistance (R), inductance (L), and capacitance (C). R denotes the Ohmic resistance in the transmission line. The total effective inductance is the sum of the inductance of the lumped element (L_c) and the distributed element (L_d), resulting in a total effective inductance of $L_c + L_d$. The resonant frequency (f_r) is determined accordingly. And the dimension of the unit cells is: a= 16 mm, b = 8 mm, c = 20 mm, g = 1 mm and h = 1.6 mm.

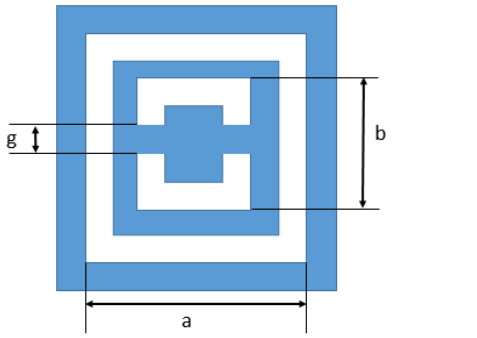

(a)

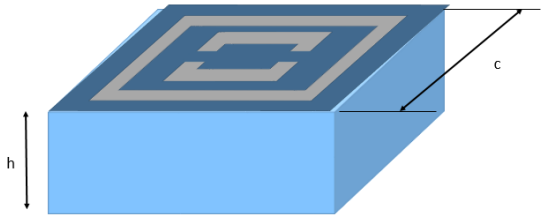

(b)

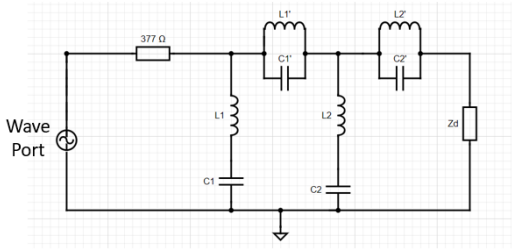

(c)

Fig. 1 (a) Top view of unit cell (b) Perspective view of unit cell and (c) Equivalent transmission line model

To verify the performance of the metamaterial-based unit cell, simulated data of the transmission coefficient S_{21} and the reflection coefficient S_{11} are used to determine the permittivity and permeability. Equations (1) and (2) are applied to calculate the relative permittivity and permeability of the MMA, given that the surface thickness is 1.6 mm. The wave period is considered as $k_o = 2f_c$, where c represents the speed of light and f is the microwave signal frequency.

$$Permittivity, \varepsilon_r = \frac{2}{j\, k_0 d} X \frac{(1 - S_{11} - S_{21})}{(1 + S_{11} + S_{21})} \quad (1)$$

$$Permeability, \mu_r = \frac{2}{j\, k_0 d} X \frac{(1 - S_{21} + S_{11})}{(1 + S_{21} - S_{11})} \quad (2)$$

Understanding the relative permittivity and relative permeability is useful for calculating the normalized impedance, Z, as specified by the equation (3)

$$Normalized\ impedance, Z = \frac{Z_{eff}}{Z_0} = \sqrt{\frac{\mu_r}{\varepsilon_r}} \quad (3)$$

where Z_{eff} is the effective impedance that includes combined effects for different portions of the MMA, and Z_o is the free space impedance that is about 377 Ω.

3 SIMULATED RESULTS AND DISCUSSION

ANSYS High-Frequency Structure Simulator (HFSS), a full-wave simulation tool, is utilized to model the proposed structure. The design featured an array of 2×2 unit cells with overall dimensions of 40 mm × 40 mm × 1.6 mm as shown in figure 2 (a). For excitation, a pair of floquet port was integrated into the design. The absorber was constructed using an FR-4 substrate with a dielectric constant of 4.4 and a loss tangent of 0.02, while the copper used had a conductivity of 5.8 × 10^7 S/m. The simulation return losses are -5.78 dB & -7.89 dB at 3 GHz and 6.9 GHz correspondingly as shown in figure 2 (b), while absorption are 73.6 % and 83.7% only as shown in figure 2 (c). In order to achieve higher absorption, optimized 2 x 4 absorber is design with the overall size of 80 mm x 40 mm x 1.6 mm as shown in figure 3 (a). The simulation return losses are -27.27 dB & -21.06 dB at 3 GHz and 6.9 GHz correspondingly as shown in figure 3 (b), while absorption are 99.8 % and 99.2 % only as shown in figure 3 (c). Furthermore, the designed absorber is compared with the already published work in table 1, which shows that proposed absorber has good absorptivity and cost effective.

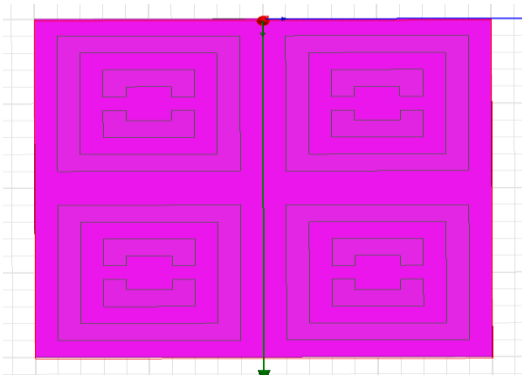

(a)

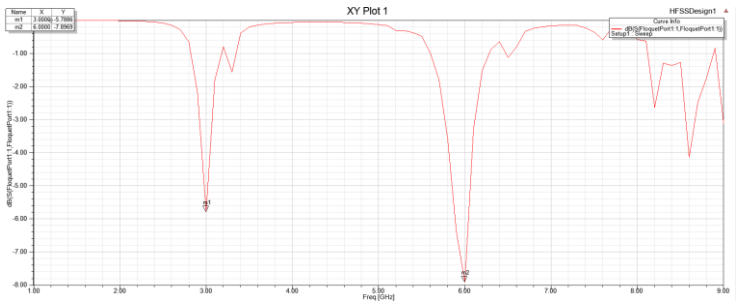

(b)

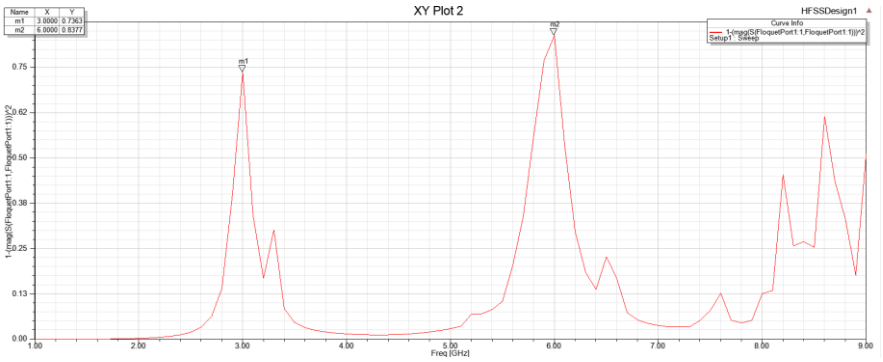

(c)

Fig. 2 Simulated result of 2x2 absorber (a) top view of proposed absorber (b) return losses and (c) absorption

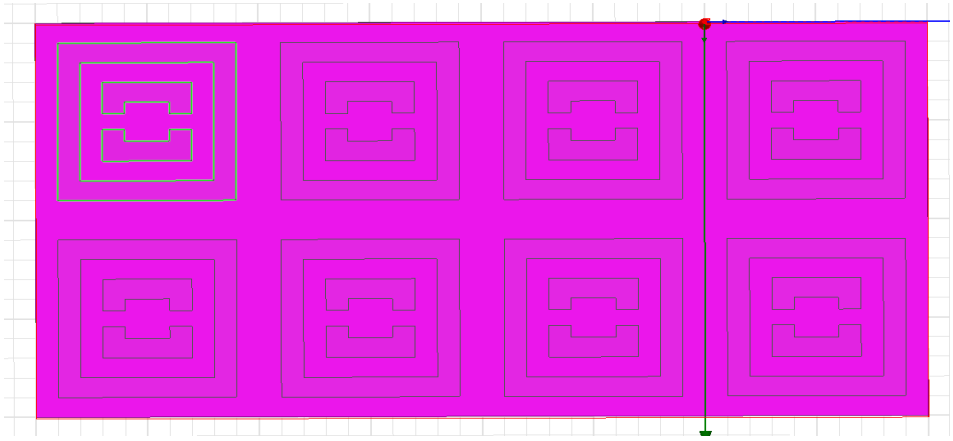

(a)

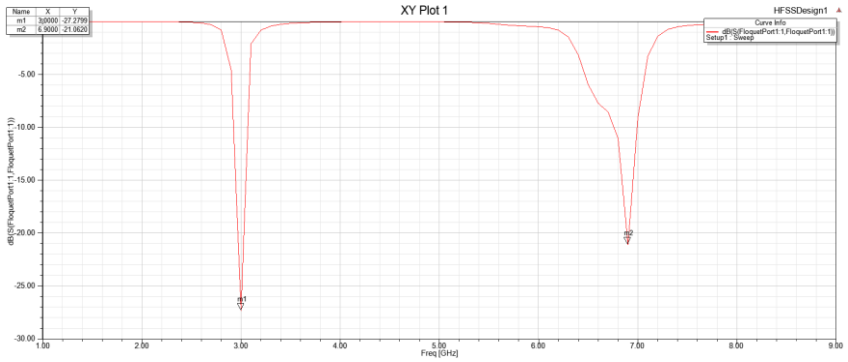

(b)

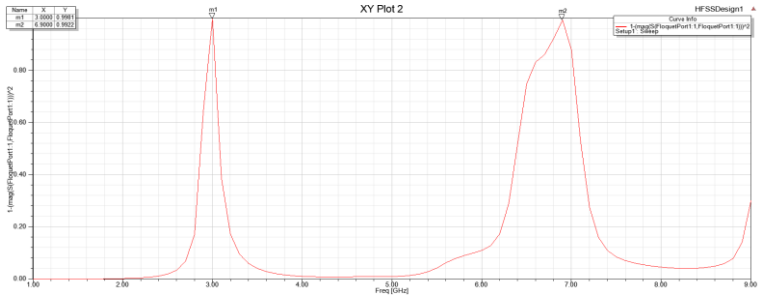

(c)

Fig. 3 Simulated result of 2x4 absorber (a) top view of proposed absorber (b) return losses and (c) absorption

Table 1: Evaluation between this work and the previous published articles

Reference	Frequency (GHz)	Absorption	Reflection coefficient S11	Thickness / substrate	Size
[15]	9.12 GHz and 11.34 GHz	99.35%, and 97.81%	NA	0.4 mm / FR-4	9 mm x 9 mm
[16]	5.95 and 12.25 GHz	> 90 % and > 90 %	NA	0.8 mm / FR-4	NA
[17]	2.4 GHz and 4.9 GHz	95.33% and 95.99%	-37 dB and -42 dB	1.575 mm / Rogers RT 5880	30 mm x 30 mm
[18]	9.68 to 17.45 GHz	90 % and 95 %	NA	1.6 mm / FR-4	NA
This work	3 GHz and.9GHz	99.8 % and 99.2 %	-27.27 dB and -21.06 dB	1.6 mm / FR-4	40 mm x 80 mm

4 HARDWARE IMPLEMENTATION RESULTS AND DISCUSSION

This section discusses, the Hardware implementation and comparative analysis of practically measured results with simulated. Following figures 4, 5 and 6 are actual images of the three different designs of 2x2, 2x4 dimensions of thickness of 0.8 and 1.6 mm respectively.

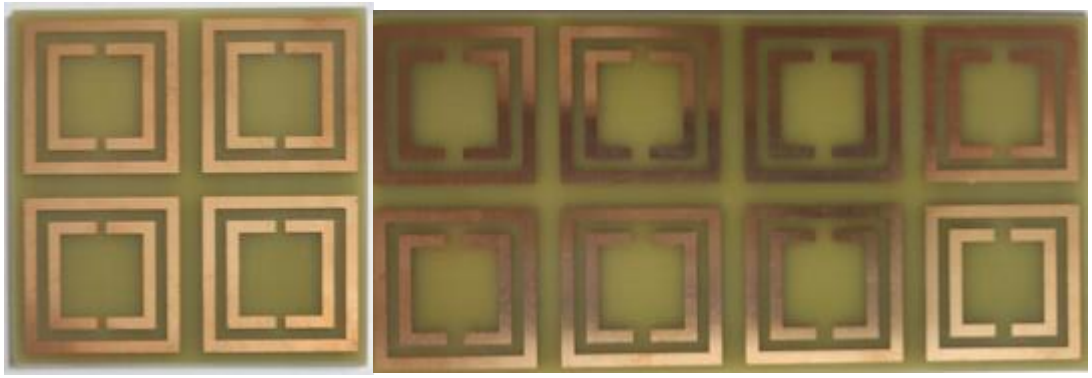

Fig. 4 Design 1 2x2 and 2x4, thickness 0.8 and 1.6

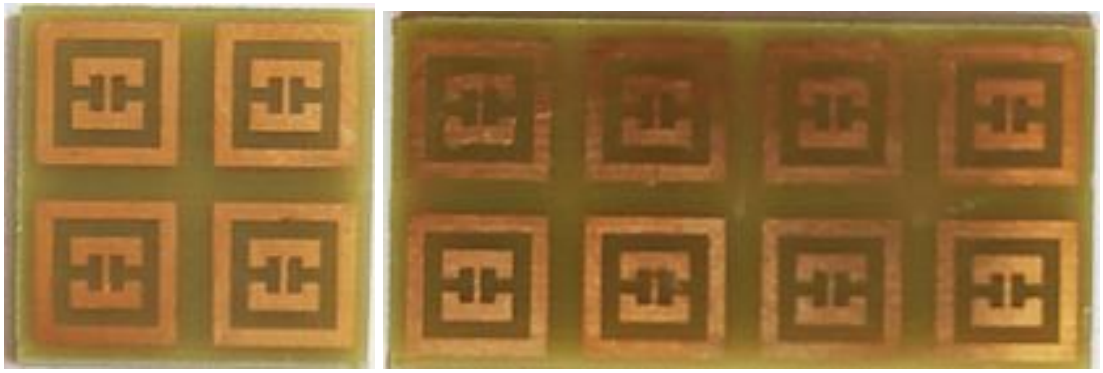

Fig. 5 Design 2 2x2 and 2x4, thickness 0.8 and 1.6

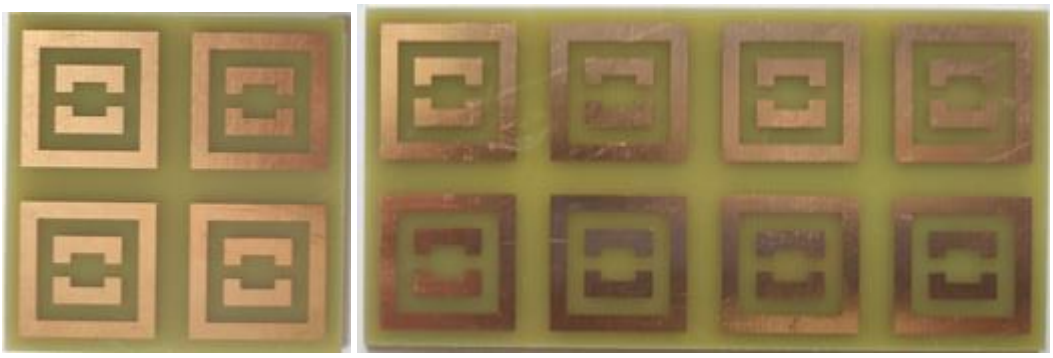

Fig. 6 Design 3 2x2 and 2x4, thickness 0.8 and 1.6

The Figures below indicates the absorptions of the three different design and summarized results in the following Table 2.

Fig. 7 Absorption Plot of Design 2x2, thickness 0.8 and 1.6

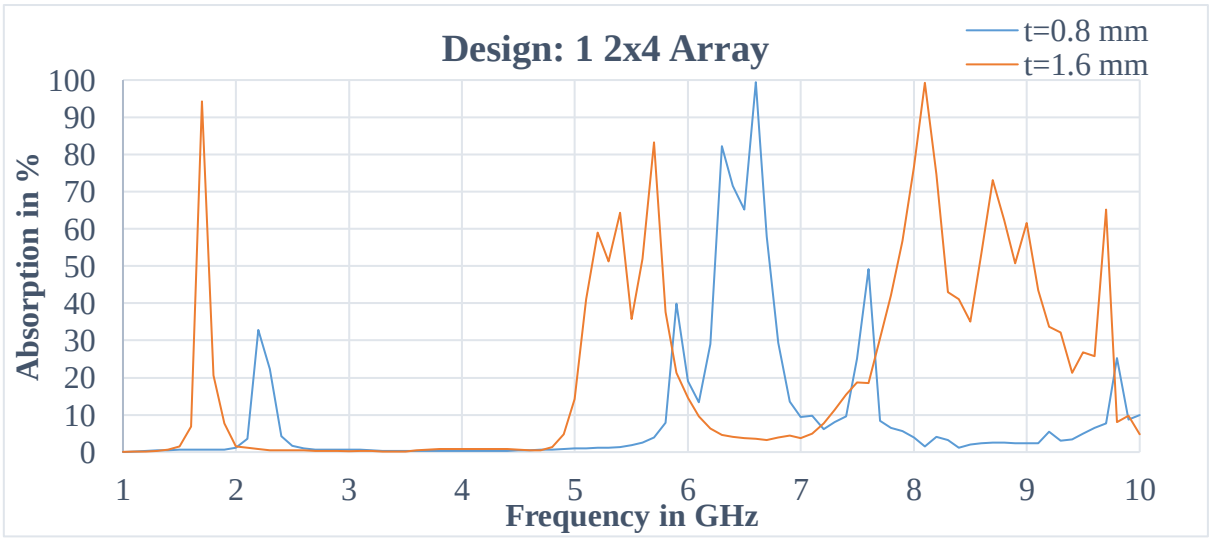

Fig. 8 Absorption Plot of Design 2x4, thickness 0.8 and 1.6

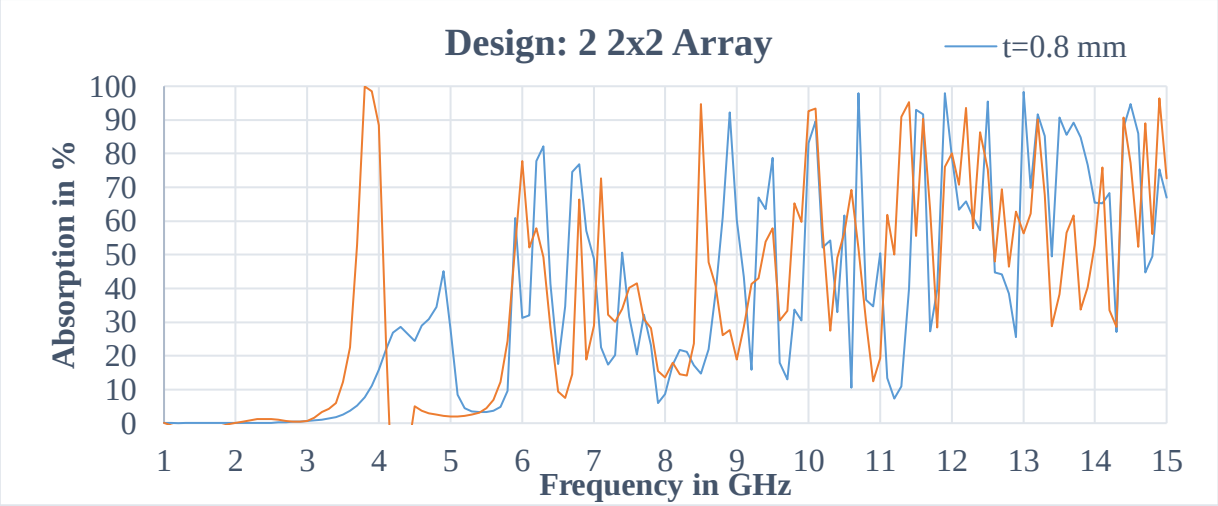

Fig. 9 Absorption Plot of Design 2x2, thickness 0.8 and 1.6

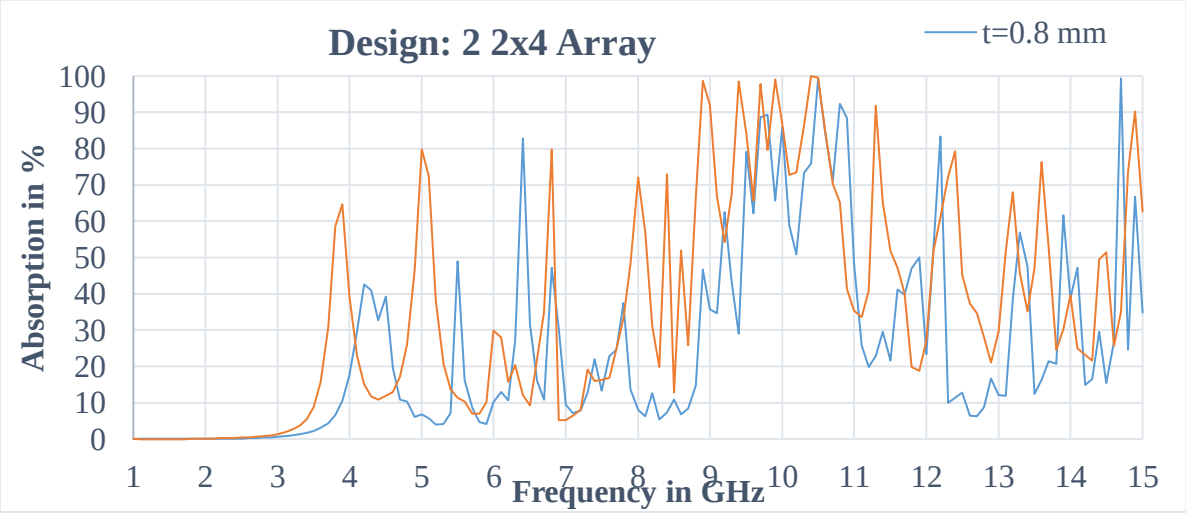

Fig. 10 Absorption Plot of Design 2x4, thickness 0.8 simulated and Practical

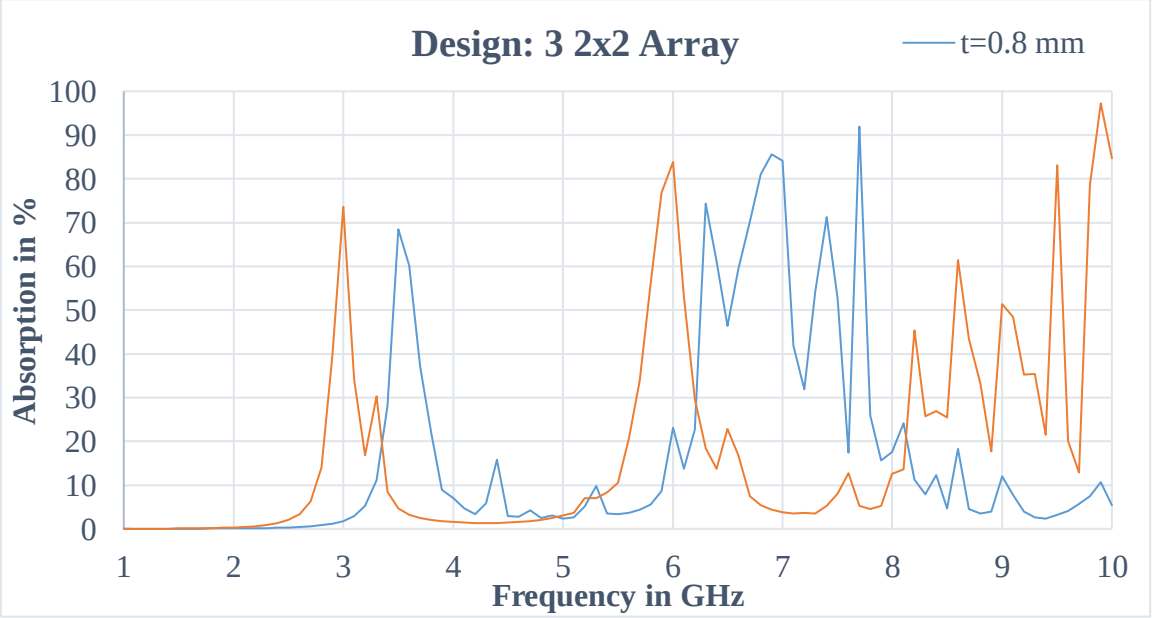

Fig. 11 Absorption Plot of Design 2x2, thickness 0.8 simulated and Practical

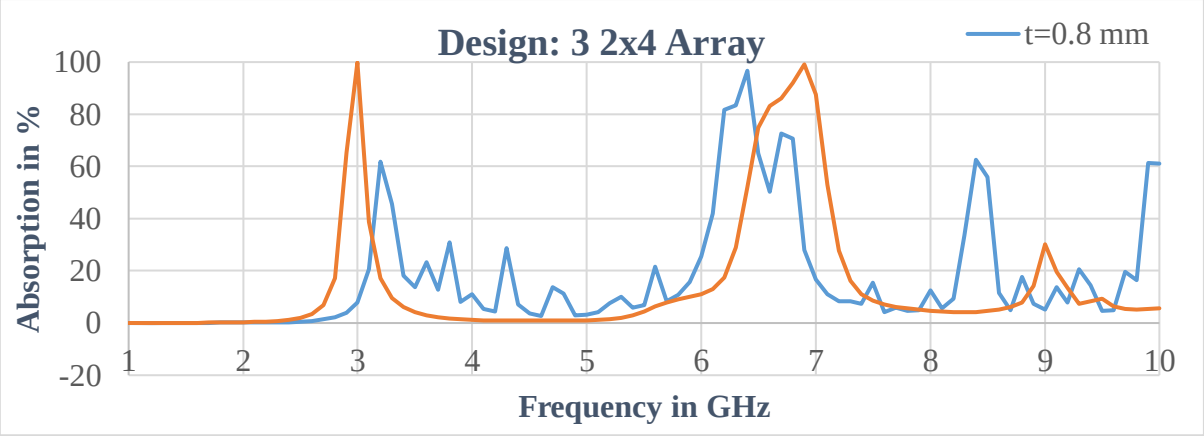

Fig. 12 Absorption Plot of Design 2x4, thickness 0.8 simulated and Practical

Table 2: Comparative Analysis of Results with different substrate

Comparative Analysis for thickness of substrate t = 1.6 mm												
	Deign - I				**Design - II**				**Design - III**			
	2x2 Array		**2x4 Array**		**2x2 Array**		**2x4 Array**		**2x2 Array**		**2x4 Array**	
	Freq. (GHz)	**A (%)**	**Freq. (GHz)**	**A (%)**	**Freq. (GHz)**	**A (%)**	**Freq. (GHz)**	**A (%)**	**Freq. (GHz)**	**A (%)**	**Freq. (GHz)**	**A (%)**
Simulated	8	95.79	1.75.6	92.78 91.12	9.5 9.9 10.5 13.3 13.9 14.4	Above 95	4.5 9.4 9.8 12.5 12.9	Above 95	3 6 9.5 9.9	73.63 83.77 83.15 97.23	3 6.9	99.81 99.22
Measured	1.7 8.2	82.62 86.84	1.7 8.1	84.07 88.23	3.8 8.5 14.9	94.62 90.08 91.39	9.7 9.9 10.4 14.9	89.87 89.18 93.47 85.56	3 5.9 9.5 9.9	63.22 72.96 78.91 85.26	3 6.9	95.17 87.97
Comparative Analysis for thickness of substrate t = 0.8 mm)												
	Deign - I				**Design - II**				**Design - III**			
	2x2 Array	**2x4 Array**	**2x2 Array**	**2x4 Array**	**2x2 Array**	**2x4 Array**	**2x2 Array**	**2x4 Array**	**2x2 Array**	**2x4 Array**	**2x2 Array**	**2x4 Array**
	Freq.	**A (%)**	**Freq.**	**A (%)**	**Freq.**	**A (%)**	**Freq.**	**A (%)**	**Freq.**	**A (%)**	**Freq.**	**A (%)**

	(GHz)		(GHz)		(GHz)		(GHz)		(GHz)		(GHz)	
Simulated	6.2	93.49	6.6	99.43	8.9 10.7 11.9 12.5 13 13.2 13.5 14.5	Above 90	10.5 10.8 14.7	Above 92	3.5 6.3 6.9 7.4 7.7	68.54 74.36 85.54 71.21 91.94	3.2 6.4 6.7 8.4 9.9	61.93 96.68 72.53 62.59 61.43

5. CONCLUSION

In this paper, a novel dual band double slit SRR (DSS) cell as an MMA unit cell designed for wide-incidence-angle absorption. The simulated return losses are -27.27 dB & -21.06 dB at 3 GHz and 6.9 GHz likewise. While the simulated absorptivity was higher than 90% for both the bands. Design was real time implemented and tested in the laboratory and measured the results is tabulated in the table 2. From the results we can conclude that, simulated and practical results are nearly same except Design-1 of 2x2 array. This makes it ideal for applications including aircraft surveillance, satellite navigation, and radar systems. Moreover, the material used in the designing of the absorber is cost effective.

Authors' Contribution

All authors contributed to the manuscript and have read and approved the final version. JP performed the literature review, JP realized the simulation and analysis, JP and RM were responsible for writing the manuscript and revisions.

Conflicts of Interest

The authors declare that there is no conflict of interest regarding the publication of this paper.

Funding Statement

This study had no funding from any resource.

Acknowledgments

We sincerely thank the E. & C. Engineering Department of BVM Engineering College, Vallabh Vidyanagar, Gujarat, India for providing lab facility for measurement of proposed metamaterial absorber.

REFERENCES

[1] Schurig, D., Mock, J. J., Justice, B. J., Cummer, S. A., Pendry, J. B., Starr, A. F., & Smith, D. R. (2006). Metamaterial electromagnetic cloak at microwave frequencies. Science, 314(5801), 977-980.

[2] Li, M., Xiao, S., Bai, Y. Y., & Wang, B. Z. (2012). An ultrathin and broadband radar absorber using resistive FSS. IEEE Antennas and Wireless Propagation Letters, 11, 748-751.

[3] Cong, L., Tan, S., Yahiaoui, R., Yan, F., Zhang, W., & Singh, R. (2015). Experimental demonstration of ultrasensitive sensing with terahertz metamaterial absorbers: A comparison with the metasurfaces. Applied Physics Letters, 106(3).

[4] Wu, C., Neuner III, B., John, J., Milder, A., Zollars, B., Savoy, S., & Shvets, G. (2012). Metamaterial-based integrated plasmonic absorber/emitter for solar thermo-photovoltaic systems. Journal of Optics, 14(2), 024005.

[5] Wang, S., & Zhan, Q. (2016). Reflection type metasurface designed for high efficiency vectorial field generation. Scientific reports, 6(1), 29626.

[6] Zhang, H. B., Zhou, P. H., Lu, H. P., Xu, Y. Q., Liang, D. F., & Deng, L. J. (2012). Resistance selection of high impedance surface absorbers for perfect and broadband absorption. IEEE Transactions on Antennas and Propagation, 61(2), 976-979

[7] Landy, N. I., Sajuyigbe, S., Mock, J. J., Smith, D. R., & Padilla, W. J. (2008). Perfect metamaterial absorber. Physical review letters, 100(20), 207402.

[8] Li, S. J., Cao, X. Y., Gao, J., Liu, T., Zheng, Y. J., & Zhang, Z. (2015). Analysis and design of three-layer perfect metamaterial-inspired absorber based on double split-serration-rings structure. IEEE Transactions on Antennas and Propagation, 63(11), 5155-5160.

[9] Ghosh, S., Bhattacharyya, S., Kaiprath, Y., & Vaibhav Srivastava, K. (2014). Bandwidth-enhanced polarization-insensitive microwave metamaterial absorber and its equivalent circuit model. Journal of Applied Physics, 115(10).

[10] Arik, K., AbdollahRamezani, S., & Khavasi, A. (2017). Polarization insensitive and broadband terahertz absorber using graphene disks. Plasmonics, 12, 393-398.

[11] Lee, J., Yoon, Y. J., & Lim, S. (2012). Ultra-thin polarization independent absorber using hexagonal interdigital metamaterial. ETRI Journal, 34(1), 126-129.

[12] Cheng, Y., Yang, H., Cheng, Z., & Wu, N. (2011). Perfect metamaterial absorber based on a split-ring-cross resonator. Applied Physics A, 102, 99-103.

[13] Nguyen, T. T., & Lim, S. (2017). Wide incidence angle-insensitive metamaterial absorber for both TE and TM polarization using eight-circular-sector. Scientific reports, 7(1), 3204.

[14] Lee, D., Hwang, J. G., Lim, D., Hara, T., & Lim, S. (2016). Incident angle-and polarization-insensitive metamaterial absorber using circular sectors. Scientific reports, 6(1), 27155.

[15] Al-Badri, K. S. L., Alwan, Y. S., & Khalaf, M. F. (2021). Ultra-thin dual-band perfect metamaterials absorber for microwave applications. Materials Today: Proceedings, 42, 2164-2168.

[16] Zhai, H., Li, Z., Li, L., & Liang, C. (2013). A dual-band wide-angle polarization-insensitive ultrathin gigahertz metamaterial absorber. Microwave and Optical Technology Letters, 55(7), 1606-1609.

[17] Bağmancı, M., Wang, L., Sabah, C., Karaaslan, M., Paul, L. C., Rani, T., & Unal, E. (2024). Broadband multi-layered stepped cone shaped metamaterial absorber for energy harvesting and stealth applications. Engineering Reports, e12903. Song, C., Wei, Y., Wang, J., Zhang, B., Qin, Y., & Duan, J. (2024). A wide-angle incidence, broadband rectified metasurface for radar frequency band EM energy harvesting and wireless power transfer. Optics & Laser Technology, 174, 110544.

[18] Patel, Jigar, & Rahul Mehta. "Simulation based Comparative Review on a Metasurface based Perfect Absorber." Journal of Advanced Engineering and Computation [Online], 7.4 (2023): 204-209.